南京航空航天大学

论文集

（二〇〇七年） 第7册

能源与动力学院

（第2分册）

南京航空航天大学科技部编

二〇〇八年三月

能源与动力学院

021 系

目录

序号	姓名	职称	单位	论文题目	刊物、会议名称	年、卷、期	类别
1	万大为 郭荣伟	博士生 正高	021 021	Exxperimental Investigation of a Fixed-geometry Two-dimensional Mixed-compression Supersonic Inlet with Sweep-forward Highlight and Bleed Slot in an Inverted "X"-type Layout	中国航空学报（英文版）	2007.20.4	
2	万大为 郭荣伟	博士生 正高	021 021	定几何二元倒置“X”型混压式超声速进气道实验	南京航空航天大学学报	2007.39.3	
3	万大为 郭荣伟	博士生 正高	021 021	定几何二元倒置“X”型混压式超声速进气道数值仿真与实验验证	航空动力学报	2007.22.8	
4	谢旅荣 郭荣伟	博士生 正高	021 021	定几何混压式轴对称超声速进气道气动特性数值仿真和实验验证	航空学报	2007.28.1	
5	谢旅荣 郭荣伟	博士生 正高	021 021	双下侧布局二元超声速进气道掺混气动特性研究	航空学报	2007.28.6	
6	谢雪明 郭荣伟	硕士生 正高	021 021	定几何混压式轴对称超声速进气道的稳定性实验	南京航空航天大学学报	2007.39.3	
7	石磊 郭荣伟	博士生 正高	021 021	蛇形进气道的电磁散射特性	航空学报	2007.28.6	
8	靖建朋 郭荣伟	博士生 正高	021 021	蛇形进气道地面工作状态附面层抽吸试验研究	南京航空航天大学学报	2007.39.1	
9	刘志友 郭荣伟	博士生 正高	021 021	航空发动机在高空台上的H0/Ma0试验分析	航空动力学报	2007.22.7	
10	周正贵 王传宝	副高 初级	021 606所	吸附式压气机叶栅气动性能计算模拟研究	航空动力学报	2007.22.12	
11	李念 张堃元	博士生 正高	021 021	应用PIV技术测量压电型自耦合射流	航空学报	2007.28.1	
12	李念 张堃元	博士生 正高	021 021	不同出口型与驱动频率的活塞型自耦合射流研究	航空动力学报	2007.22.3	
13	孙波 张堃元	博士生 正高	021 021	流线追踪Busemann进气道马赫数3.85实验研究	航空动力学报	2007.22.3	
14	孙波 张堃元	博士生 正高	021 021	流线追踪Busemann进气道设计参数的选择	推进技术	2007.28.1	
15	潘瑾 张堃元	博士生 正高	021 021	可变内收缩比侧压式进气道自起动性能	推进技术	2007.28.3	
16	骆晓臣 张堃元	博士生 正高	021 021	侧压式进气道附加阻力分析	推进技术	2007.28.6	
17	骆晓臣 张堃元	博士生 正高	021 021	侧压式进气道内部阻力的参数分析	推进技术	2007.28.3	
18	骆晓臣 张堃元	博士生 正高	021 021	侧压式进气道内部阻力分析	推进技术	2007.28.2	
19	张堃元 居燕 杨国亮 金志光	正高 中级 硕士生 中级	021 金城集团 021 021	曲面激波压缩和在高超声速进气道上的应用	中国力学学会学术会议	2007.6	

目录

序号	姓名	职称	单位	论文题目	刊物、会议名称	年、卷、期	类别
20	叶飞 张堃元	硕士生 正高	021 021	进气道出口旋流模拟研究	中国航空学会推进系统气动热力学专业第十一届学术会议	2007.07	
21	陈秋华 张堃元	硕士生 正高	021 021	喉道处排除顶板附面层对侧压式进气道起动性能影响的实验研究	第二届冲压发动机学术会议	2007.9	
22	郭敬涛 张堃元	硕士生 正高	021 021	颌下进气道攻角性能研究	第二届冲压发动机学术会议	2007.9	
23	曹学斌 张堃元	硕士生 正高	021 021	非对称来流下超燃冲压发动机隔离段动态压力研究	第二届冲压发动机学术会议	2007.9	
24	金志光 张堃元	博士生 正高	021 021	二元高超声速进气道与侧压式进气道的性能比较	第二届冲压发动机学术会议	2007.9	
25	孙波 张堃元	博士生 正高	021 021	弹用模块化Busemann进气道研究	第二届冲压发动机学术会议	2007.9	
26	南向军 孙波 张堃元	硕士生 博士生 正高	021 021 021	弹用Busemann进气道初步研究	第二届冲压发动机学术会议	2007.9	
27	尹智 张堃元	硕士生 正高	021 021	乘波前体/侧压式进气道一体化设计初步研究	第二届冲压发动机学术会议	2007.9	
28	杨国亮 张堃元	硕士生 正高	021 021	曲面侧板压缩的侧压式进气道研究	第二届冲压发动机学术会议	2007.9	
29	潘瑾 张堃元	博士生 正高	021 021	前体来流条件对侧压式进气道性能影响	第二届冲压发动机学术会议	2007.9	
30	孙波 张堃元	博士生 正高	021 021	CFD Analysis of modular hypersonic Busemann	ISABE会议	2007.	
31	骆晓臣 张堃元	博士生 正高	021 021	Analysis of additive drag in sidewall-compression inlet	ISABE会议	2007.	
32	骆晓臣 张堃元	博士生 正高	021 021	隔离段内超声速流动摩擦阻力分析	第二届冲压发动机学术会议	2007.9	
33	徐惊雷 李超 沙江 张堃元	副高 硕士生 硕士生 正高	021 021 021 021	多压电膜式零质量射流激励器的设计与性能研究	航空动力学报	2007.22.11	
34	徐惊雷 张艳慧 张堃元	副高 硕士生 正高	021 021 021	超燃冲压发动机非对称喷管非设计状态性能数值计算	推进技术	2007.28.3	
35	徐惊雷 沙江 林春峰 张堃元	副高 硕士生 硕士生 正高	021 021 021 021	不同狭缝厚度的零质量射流PIV实验研究	推进技术	2007.28.2	
36	徐惊雷	副高	021	径向运动方程在绝对与相对坐标系下的相互转换	力学与实践	2007.29.6	
37	徐惊雷 沙江 林春峰 张堃元	副高 硕士生 硕士生 正高	021 021 021 021	The PIV Experimental Research of Instataneous Flow Characteristics of Circular Orifice Synthetic Jet	Journal of Hydrodynamics, Ser.B	2007.19.4	

目录

序号	姓名	职称	单位	论文题目	刊物、会议名称	年、卷、期	类别
38	徐惊雷 李超 沙江 张堃元	副高 硕士生 硕士生 正高	021 021 021 021	The Design and Experimental Study of Multi-Diaphragm Piezoelectric Synthetic Jet Actuator, IMECE 2007-43193	ASME International Mechanical Engineering Congress and Exposition(IMECE), 2007	2007	
39	张艳慧 徐惊雷 张堃元	硕士生 副高 正高	021 021 021	超燃冲压发动机非对称喷管设计及设计点性能研究	推进技术	2007.28.3	
40	沙江 徐惊雷 林春峰 张堃元	硕士生 副高 硕士生 正高	021 021 021 021	双圆形出口零质量射流组的流场结构PIV实验	航空动力学报	2007.22.4	

Available online at www.sciencedirect.com
ScienceDirect
Chinese Journal of Aeronautics 20(2007) 304-312
Chinese Journal of Aeronautics
www.elsevier.com/locate/cja

Experimental Investigation of a Fixed-geometry Two-dimensional Mixed-compression Supersonic Inlet with Sweep-forward High-light and Bleed Slot in an Inverted "X"-type Layout

Wan Dawei*, Guo Rongwei

College of Energy and Power Engineering, Nanjing University of Aeronautics and Astronautics, Nanjing 210016, China

Received 19 September 2006; accepted 11 May 2006

Abstract

A fixed-geometry two-dimensional mixed-compression supersonic inlet with sweep-forward high-light and bleed slot in an inverted "X"-form layout was tested in a wind tunnel. Results indicate: (1) with increases of the free stream Mach number, the total pressure recovery decreases, while the mass flow ratio increases to the maximum at the design point and then decreases; (2) when the angle of attack, α, is less than 6°, the total pressure recovery of both side inlets tends to decrease, but, on the lee side inlet, its values are higher than those on the windward side inlet, and the mass flow ratio on lee side inlet increases first and then falls, while on the windward side it keeps declining slowly with the sum of mass flow on both sides remaining almost constant; (3) with the attack angle, α, rising from 6° to 9°, both total pressure recovery and mass flow ratio on the lee side inlet fall quickly, but on the windward side inlet can be observed decreases in the total pressure recovery and increases in the mass flow ratio; (4) by comparing the velocity and back pressure character- ristics of the inlet with a bleed slot to those of the inlet without, it stands to reason that the existence of a bleed slot has not only widened the steady working range of inlet, but also made an enormous improvement in its performance at high Mach numbers. Besides, this paper also presents an example to show how this type of inlet is designed.

Keywords: aerospace propulsion system; supersonic inlet; two-dimensional mixed-compression; experimental investigation; bleed slot; "X"-type; sweep-forward high-light

1 Introduction

The mixed-compression inlet has attracted the researchers in this area due to its smaller external drag, better performance and inherent aerodynamic characteristics that make it capable of working in a wider range. Therefore, it is very important to study its design approach and improvement thereof th- rough a variety of configurations and layouts.

Lots of research on the mixed-compression supersonic inlet were conducted since the 1950s[1]. As a feasible solution, inlets of variable geometry, generally with boundary layer bleed/suction system, came in wide use in some aircrafts, such as the American SR-71. However, so far applications are rarely found in missiles because of the complexity of its structure. In this paper, investigations on the boundary layer bleed/suction system are carried out for the purpose of finding an easy way to improve the missile inlet. Ref.[2] demonstrates the design procedure of a boundary-layer bleed system for supersonic inlets with emphasis on the selection of bleed hole geometry. Experimental bleed hole performance data coupled with bleed drag calculations show that holes with shallow inclination are superior to those which are normal to

*Corresponding author. Tel.: +86-25-84892203-2415.
E-mail address: waste_wan@163.com

the surface in terms of overall inlet performance. In Ref.[3], experimental investigations of mixed-compression inlets with the design point of Ma=3.00 were performed. The results indicate that the ramp bleed is significant for starting and pressure recovery, so is the cowl bleed system for suppressing flow separation and vortex development. In Ref.[4], an analytical model of boundary-layer bleed holes and slots for supersonic inlets was developed. However, although the works mentioned above have paid close attention to the mechanism or characteristics of boundary-layer bleed/suction system, applications on the missiles have not been found yet. In addition, numerical studies of the mixed-compression inlets on missiles of different configurations were performed in Refs.[5-7]. An experimental investigation of a missile inlet with an inverted "X"-type configuration was conducted in Ref.[8]. Similarly, these researches are mostly concerned with the inherent characteristics of the inlet, and the improvement of inlet performance through its configuration did not attract much interest.

In this paper, a fixed-geometry two dimensional mixed compression supersonic inlet with sweep-forward high-light and bleed slot with an inverted "X"-type configuration has been worked out and tested in a wind tunnel. Results show that when the angle of attack is less than 6°, the inlet has good aerodynamic characteristics in terms of total pressure coefficients and mass flow ratios. Besides, in comparison with the inlet without a bleed slot, the performance of the inlet with a slot is better, in particular, at high Mach numbers and its stable working range is considerably extended. The present study is experimentally helpful to the design of this type of inlet and its further amelioration.

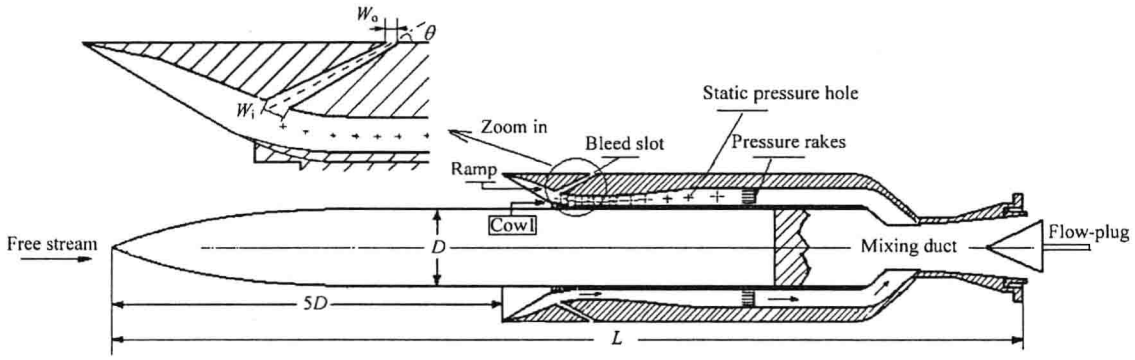

Fig.1 Sketch of the inlet model.

2 Test Model and Tunnel

A two-dimensional fixed-geometry mixed-compression inlet with a bleed slot in the shoulder area of the ramp surface is made for the test. The design point of the inlet is chosen as Ma=3.00. The corresponding minimum starting Mach number and maximum working Mach number of the inlet are 2.25 and 3.50 respectively. Deflective angles of the two stage ramps are 10° and 17° to the horizon, while the reflective angle of the internal surface of the cowl near the lip is 9° to the same plane. Ratio of the capture to the throat height is about 2.45. The centerline of the slot has an angle of inclination of about 30° to the horizon. Width of the slot entrance is 0.675 times the height of the throat. The area ratio of the exit to the entrance of the slot is about 0.75. An equivalence angle of 3.5° is chosen to avoid flow separation on the surface of the diffuser.

2.1 Test model

Just as the inlet model shows in Fig.1, it is designed with a sweep-forward high-light inverted "X"-type configuration. There are four inlets located symmetrically around the body. The distance from the very begin of the inlet ramp to the body nose is

about 5*D*, where *D* is the diameter of the body. In order to be able to compare the characteristics of the present model to those of the model introduced in Ref.[8], the two models adopt an identical capture configuration.

In order to simulate the pressure variation in combustion chamber, a movable flow-plug is employed at the exit of the mixing duct. In addition, pressure rakes are aligned in the exit plane of the inlet to measure total pressure recovery and mass flow. Pressure taps are installed along the centerline of the ramp side wall to measure the static pressure distribution.

2.2 Experimental device

Tests were performed in the NH-1 blow-down wind tunnel of Nanjing University of Aeronautics and Astronautics. The mainstream Mach number of the NH-1 wind tunnel can be adjusted from 0.30 to 3.50 by replacement of nozzles. The test section is 0.6 m×0.6 m square. In order to acquire Schlieren photographs and obverse the flow filed, two windows in the form of Ø230 mm are located on both sidewalls of the section.

During the tests, the unit Reynolds number of the wind tunnel is about 3×10^7. The blockage of the model to the tunnel is about 3.4%. Fig.2 shows the model in the wind tunnel.

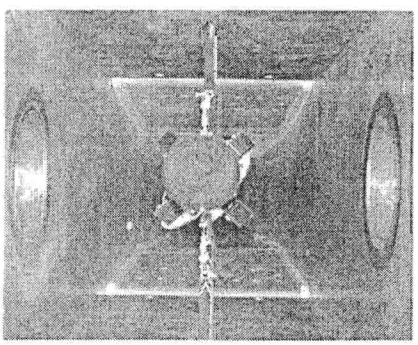

Fig.2 Model in wind tunnel.

3 Experimental Results and Discussions

The tests provide the performances of the inlet, which are evaluated by the total pressure recovery, σ, and the mass flow ratio, ϕ. Corresponding results and analyses are presented as follows.

3.1 Back pressure characteristics of the inlet

During the design of ramjet engines, the back pressure characteristics should be understood in order to ensure the working compatibility between the inlet and the combustion chamber. In Fig.3 and Fig.4, the total pressure coefficient and the mass flow ratio under the design condition (Ma = 3.00, α= 0°, β= 0°, γ= 45°) are plotted as a function of the back pressure. Values on the *Y*-axis are normalized by the corresponding value of the critical state. The *X*-coordinate, back pressure $\overline{P_b}$, denotes ratios of P_b to P_{bc}, where P_b is the ratio of the pressure at the outlet of the inlet to the pressure of free stream, and P_{bc} is the value of P_b at the critical state of the inlet. The arrows in the curve indicate the moving direction of the flow-plug from opening to closure. As shown in the figures, when the inlet is in starting state, the mass flow ratio keeps constant with the increase of the back pressure, while the total pressure recovery coefficient decreases firstly and then

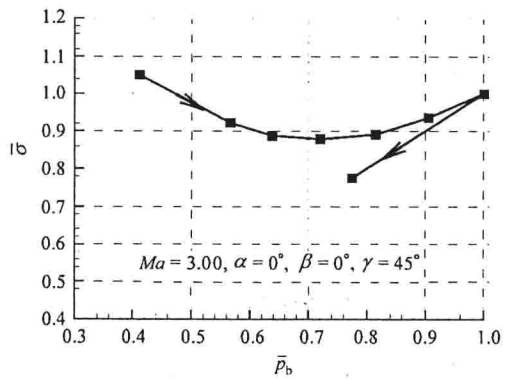

Fig.3 Total pressure recovery coefficient versus back pressure.

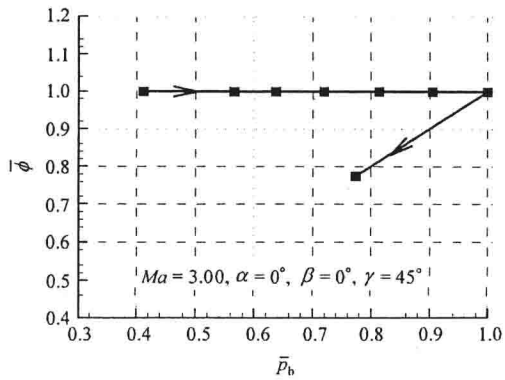

Fig.4 Mass flow ratio versus back pressure.

increases. This can be explained as follows: (1) when the flow plug is opened enough, the inlet is filled with supersonic flow so that the back pressure of the inlet is very low and the corresponding total pressure recovery coefficient keeps high; (2) as the back pressure of the inlet increases gradually, a terminal shock train crosses the measurement section in the diffuser of the inlet making the total pressure recovery coefficient decline; (3) with further increase of the back pressure, the terminal shock train moves forward and the total pressure loss of the shock drops because fore-shock Mach number becomes lower then the total pressure recovery coefficient rises. But it can be seen from Fig.3 and Fig.4 that when the plug is over moved, the total pressure recovery, the mass flow ratio and the back pressure will sharply drop which is attributed to the inlet turning into the sub-critical state with a shock occurring ahead of the inlet lip.

2.2 Velocity characteristics

The variation of the normalized total pressure recovery coefficient of the inlet against the Mach number of free stream is presented in Fig.5, which shows that the total pressure recovery coefficient descends with the increase of the Mach number of free stream. When the Mach number of free stream is larger than the design Mach number, the recovery coefficient slumps. As shown in the Fig.5, the total pressure recovery coefficient at $Ma = 3.50$ is only 40% of that at $Ma = 2.25$. The reason is probably that the outside oblique shocks intersect into the duct, which leads to the slipstream layer to enter the inlet. Additionally, the strong shocks, caused by the outside intersected oblique shocks, interact with the boundary layer to form a flow separation near the inlet lip and result in more total pressure loss.

Fig.6 illustrates the effects of the Mach number of free stream on the mass flow ratio. Y-coordinate is the ratio of the mass flow ratio at each Mach number to that at $Ma = 3.00$ Obviously, with the Mach number of free stream varying from $Ma = 2.25$ to $Ma = 3.00$, the mass flow ratio keeps ascending until its maximum obtained at the design

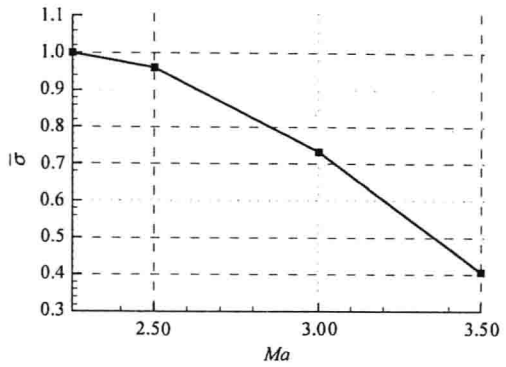

Fig.5 Total pressure recovery coefficient versus flight Mach number.

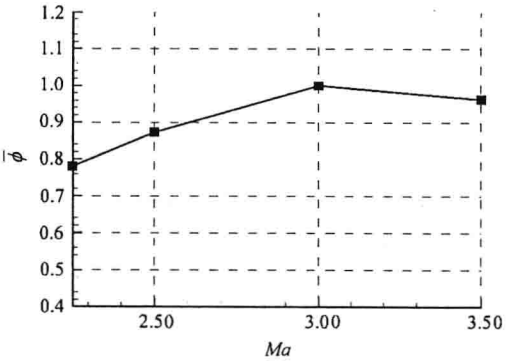

Fig.6 Mass flow ratio versus flight Mach number.

point of $Ma = 3.00$. Nevertheless, when the Mach number of free stream exceeds $Ma = 3.00$, the mass flow ratio begins declining, attributable possibly to the increase of the total pressure loss around the body nose.

3.3 Characteristics of the angle of attack

The effects of the angle of attack on the total pressure recovery coefficient are presented in Fig.7, in which the values of the pressure recovery on Y-axis are also normalized by those at $\alpha = 0°$. In this paper, a lee side inlet is defined as the inlet on the lee side of the body, and, the same way, a windward side inlet on the windward side of the body. Here, a decline of the pressure recovery can be found with the ascent of the angle of attack. However, when the angle of attack is less than 6°, the total pressure recovery decreases slowly. Also, the pressure recovery of the lee side inlet turns up slightly greater than that of the windward side inlet when the angle of attack lies below 6°. With further increases of the angle of attack, a low energy air of the lee side of the body enters the inlet of that side

resulting in a rapid drop of pressure recovery. At the angle of attack being 9°, the total pressure recovery of the lee side inlet is far lower than that of the windward side inlet.

The mass flow ratio of both side inlets is plotted against the angle of attack in Fig.8, in which the value of the mass flow ratio on *Y*-axis is normalized by that at $\alpha = 0°$. It could be seen that when the angle of attack rises to 3°, the mass flow ratio of the lee side inlet increases, while that of the windward side inlet decreases. The mass flow ratio of both side inlets drops slowly while α ranges from 3° to 6°. With further increases of the angle of attack, the mass flow ratio of the windward side inlet begins to ascend in contrast to sharply dropping in the lee side inlet. At the angle of attack of 9°, the mass flow ratio of the windward side inlet is far higher than that of the lee side inlet. It is probably because of the different development of the outside oblique shocks in both side inlets. Also, the asymmetric boundary layer around the body serves to strengthen the tendency. However, the sum of the mass flow ratios of both side inlets remains almost the same in the present study.

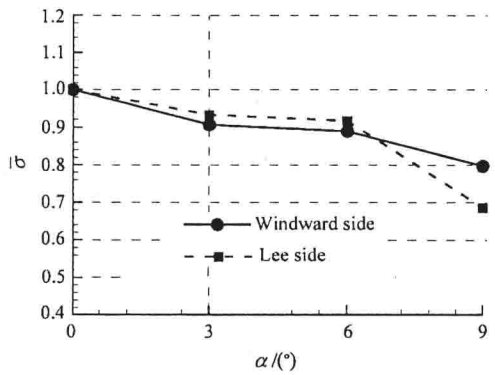

Fig.7 Total pressure recovery coefficient versus angle of attack (*Ma*=3.00).

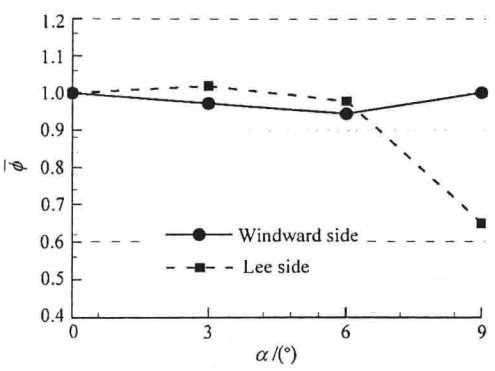

Fig.8 Mass flow ratio versus angle of attack (*Ma*=3.00).

3.4 Static pressure distribution along the inlet wall

A static pressure distribution can not only describe the variation of the static pressure but also express the shock pattern in the duct. An analysis of the static pressure distribution has been carried out to discover the rules of the performance of the inlet.

Fig.9 demonstrates the changes of the static pressure distribution against the positions of the flow plug at $Ma = 3.00$ and $\alpha = 0°$. Accordingly, the values on *Y*-axis in Fig.9 are ratios of the static pressure at each static tap to the maximum value in the changing process. Positions of the flow-plug here are marked by ID_1 to ID_8. It can be found that the inlet is in supercritical state when the curves corresponding to the positions of the plug transfer from ID_1 to ID_6. In this process, a constant mass flow ratio can be observed because the shocks at the entrance of the inlet remain unchanged while the terminal shock keeps moving forward. When the inlet enters the critical state, the terminal shock stays near the throat, which corresponds to the curve marked by ID_7 resulting in the maximum back pressure. With the plug moving onward, as is shown by ID_8, the inlet is in sub-critical state, where the back pressure, the total pressure recovery and the mass flow ratios decline in common with what has been analyzed above.

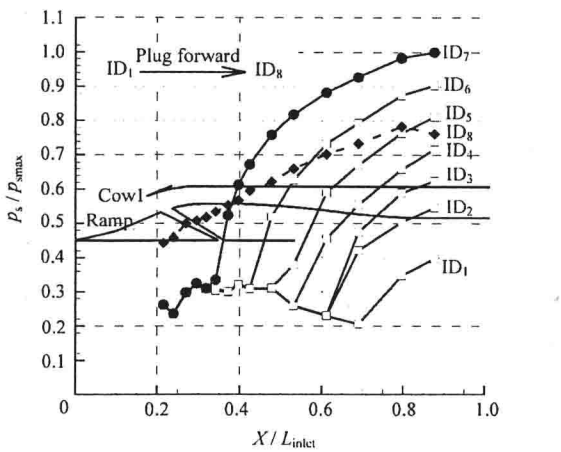

Fig.9 Static pressure ratio along the duct versus position of the plug (*Ma*=3.00, α=0°).

The static pressure distribution at $Ma = 2.50$ and $\alpha = 0°$ is presented in Fig.10, in which the curves of the static pressure distribution in the critical state of the inlet disappear because of the limited positions of the flow-plug. The state of the inlet leaps directly from the supercritical (ID_1 to ID_4) into the sub-critical (ID_5) with the plug moving forward. It can be found that the terminal shock stays at the rear edge of the slot which allows a little amount of air to escape from the slot. However, the pressure at the exit plane continues increasing. With further movement of the plug, as shown by the curve ID_6, though the terminal shock still stays within the range of the slot, it is a little bit ahead of where it was as shown by curve ID_5, leading to a maximum back pressure. It is expected that the air escaping from the slot increases and the mass flow ratio decreases. Moreover, as shown by ID_7, with the plug moving forward, the terminal shock goes out of the duct causing spillage to appear on the lip of the inlet and the back pressure to decrease. Therefore, it can be concluded that when the back pressure is slightly higher than the critical pressure of the inlet, owing to the existence of the slot, the terminal shock will stay at the entrance of the slot making it possible to extend steady working range of the inlet.

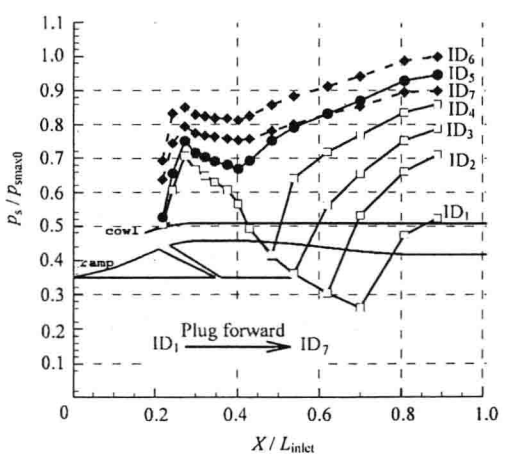

Fig.10 Static pressure ratio along the duct versus position of the plug (Ma=2.50, α=0°).

3.5 Effects of the bleed slot on the performance of the inlet

In order to determine the effects of the bleed slot on the performance of the inlet, an experimental comparison between two kinds of inlet—inlet *A* (without a bleed slot) and inlet *B* (with a bleed slot)—is made at the same capture area. Both inlets satisfy the demands on the mass flow rate of the engine.

(1) Comparison between velocity characteristics

The variations in the total pressure recovery coefficient of both inlets as function of the free stream Mach number are shown in Fig.11, where the dashed line represents the inlet *A* while the solid the inlet *B*. From the figure, the total pressure recovery coefficient of inlet *B* is higher than that of inlet *A*. This is because the throat area required to start inlet *B* decreases due to the usage of the slot, and the removal of part of the boundary layer on the ramp surface from the slot.

Fig.12 illustrates the variation of mass flow ratio of both inlets as function of the free stream Mach numbers. It appears that the mass flow ratio of the inlet *A* is higher than that of the inlet *B* when the free stream Mach number is below the design one. The difference between the mass flow ratios of the two inlets becomes all the smaller with the Mach number of free stream rising. And when the free stream Mach number becomes higher than the design one, the mass flow ratios of both inlets approach almost equal.

From Fig.11 and Fig.12, it can be observed: (1) when the free stream Mach number is below the design one, the performance of the inlet *B* is almost

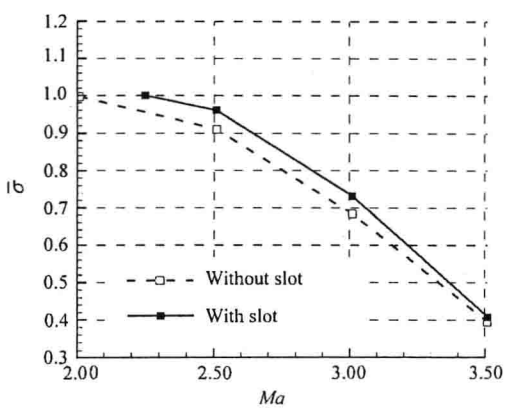

Fig.11 Total pressure recovery coefficient versus flight Mach number.

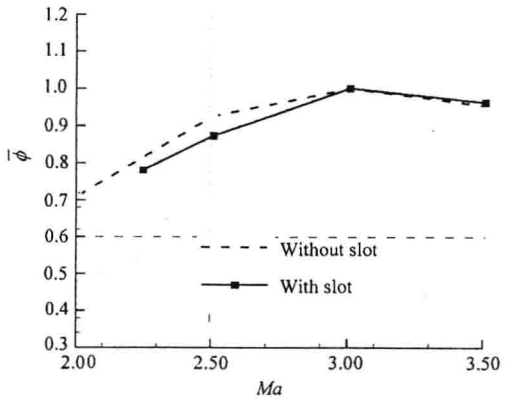

Fig.12 Mass flow ratios versus flight Mach number.

the same as that of the inlet *A* although the total pressure recovery of the inlet *B* is higher than that of the inlet *A*, yet the mass flow ratio of the inlet *B* lower than that of the inlet *A*; (2) when the Mach number of free stream is equal to or higher than the design one, the inlet *B* holds a remarkable advantage in the performance over the inlet *A* because the total pressure recovery of the inlet *B* is higher than that of the inlet *A* with the mass flow ratios of both inlets about the same. As a result, the inlet with a slot (inlet *B*) outperforms the inlet without a slot (inlet *A*).

(2) Comparison between back pressure characteristics of inlet *A* and inlet *B*

In order to give an overview of the performance of the inlet *A* and inlet *B*, a comparison of back pressure characteristics between both inlets is made as follows.

① Comparison of back pressure characteristics at $Ma = 2.5$

The total pressure recovery coefficient and the mass flow ratios as a function of the back pressures are graphed in Fig.13 and Fig.14, in which dashed lines represent the inlet *A* and solid lines the inlet *B*. Obviously, the maximum back pressure of the inlet *B* is higher than that of the inlet *A*, ascribed to a wider working range possessed by the inlet *B*. From Fig.13, it can be seen that the total pressure recovery coefficient of the inlet *B* is higher than that of the inlet *A* in the critical state. In the supercritical state, when both inlets have identical back pressure ratios within the range of 0.67 and 0.86, the inlet *A* has bigger values of the total pressure recovery. Also, in Fig.14, it is found that the mass flow ratio of the inlet *A* is larger than that of the inlet *B* under the same back pressure ranging from 0.67 to 0.86. Therefore, it is reasonable that when the speed of free stream is below the design Mach number, the inlet *A* is more suitable for working under a lower combustion pressure while the inlet *B* proves superior if the engine is working under a high back pressure.

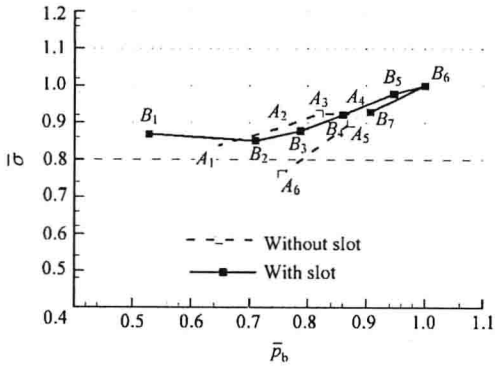

Fig.13 Total pressure recovery coefficient versus back pressure (Ma=2.50, α=0°).

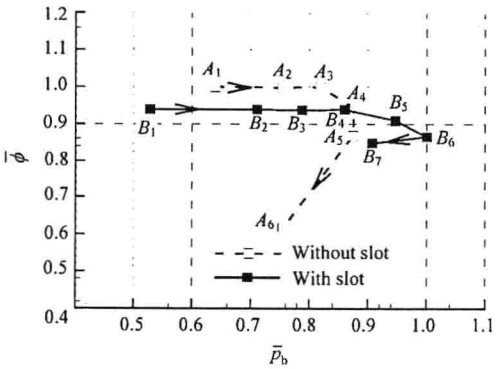

Fig.14 Mass flow ratio versus back pressure (Ma=2.50, α=0°).

② Comparison between back pressure characteristics at $Ma = 3.00$

Both Fig.15 and Fig.16 describe the variation of the total pressure recovery coefficient and the mass flow ratios of both inlets against the back pressure at $Ma = 3.00$ and α=0°. Compared to the inlet *A*, the inlet *B* has a wider working range. As presented in Fig.15, the total pressure recovery of the inlet *B* is always higher than that of the inlet *A* under the same back pressure. In Fig.16, the mass flow ratios of the inlet *B* almost equals to that of the

inlet A. Therefore, it can be concluded that the inlet B is more suitable for working at high Mach numbers.

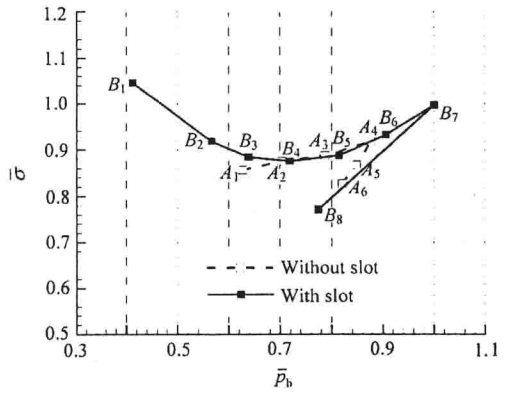

Fig.15 Total pressure recovery coefficient versus back pressure (Ma=3.00, α=0°).

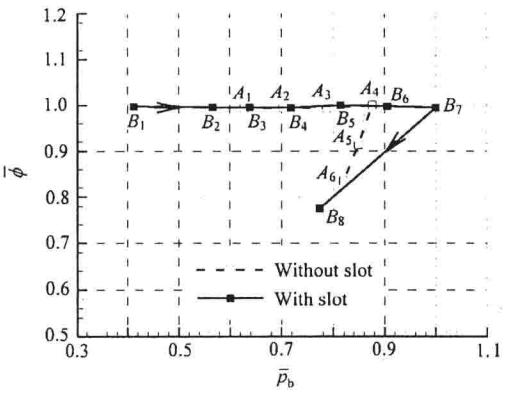

Fig.16 Mass flow ratios versus back pressure (Ma=3.00, α=0°).

4 Conclusions

An experimental study has been conducted on a fixed-geometry two-dimensional mixed-compression supersonic inlet with a sweep-forward high- light and bleed slot in an inverted "X"-type layout. The conclusions drawn from this study can be summarized as follows:

(1) With the Mach number of the free stream rising, the total pressure recovery coefficient of inlet decreases, especially when the speed of free stream is higher than the design Mach number. In contrast, the mass flow ratios increase firstly and then decrease as soon as the maximum value is achieved at the design Mach number.

(2) With ascent of the angle of attack, the mass flow ratios of both side inlets decrease. Nevertheless, the total pressure recovery of the lee side inlet is higher than that of the windward side inlet when the angle of attack is below 6°. When α varies from 6° to 9°, the total pressure recovery of the lee side inlet drops sharply. Moreover, the mass flow ratios of the lee side inlet ascend at the beginning and then descend if the angle of attack is less than 6°, while that of the windward side inlet keeps decreasing. However, the sum of the mass flow ratios of both side inlets remains almost constant. With the attack angle rising from 6° to 9°, the mass flow ratios of the lee side inlet falls quickly while that of the windward side inlet increases a little. Generally, the perfor- mance of the inlet in this study is insensitive to the angle of attack, especially when $\alpha \leqslant 6°$.

(3) The total pressure recovery coefficient of the inlet with a bleed slot is higher than that of the inlet without a bleed slot within the studied region of Mach number. As for the mass flow ratios of the two kinds of inlet, with the ascent of the free stream Mach number, they become all the closer. And as the free stream Mach number reaches or exceeds the design one, they are almost the same. So, the inlet with a bleed slot proves superior to the inlet without a bleed slot in performance at higher Mach numbers.

(4) When the free stream Mach number is below the design one, the inlet without a bleed slot is more suitable for working under lower back pressure which the engine is working at. It is true of the inlet with a bleed slot under high back pressure. At the design Mach number, the inlet with a bleed slot outperforms the inlet without.

(5) Analysis on the static pressure distribution along the inlet wall shows that the terminal shock can be made stay at the slot entrance by a bleed slot resulting in an extension of working range of the inlet.

References

[1] Goldsmith E L, Seddon J. Practical intake aerodynamic design. Cambridge: Blackwell Scientific Publications, 1993.

[2] Syberg J, Koncsek L. Bleed system design technology for supersonic inlets. AIAA 72-1138, 1972.

[3] Murakami A, Yanagi R. Mach 3 wind tunnel test of mixed compression supersonic inlet. AIAA 92-3625, 1992.

[4] Gary J, Gregory E. On supersonic-inlet boundary-layer bleed flow. AIAA 95-0038, 1995.

[5] Xie L R, Guo R W. Numerical simulation and experimental validation of the flow in a mixed-compression axisymmetric supersonic inlet with fixed-geometry. Acta Aeronautica et Astronautica Sinica 2007; 28(1): 78-83. [in Chinese]

[6] Li B, Liang D W. Computation of the integrated flow field around missile and mixed compression intake. Journal of Propulsion Technology 2002; 23(4): 307-310. [in Chinese]

[7] Bai P, Zhu S M. The numerical study of the effect of the angle of attack of the missile ramjet in the "X" type configuration. Journal of Astronautics 2005; 26(1): 99-103. [in Chinese]

[8] Wan D W, Guo R W. Experiment on fixed-geometry two-dimensional mixed-compression supersonic inlet with sweep forward high-light and "X"-type missile configuration. Journal of Nanjing University of Aeronautics and Astronautics 2007; 39(3): 277-281. [in Chinese]

Biography:

Wan Dawei Born in 1979, he is a Ph.D. candidate at Nanjing University of Aeronautics and Astronautics. His research interest covers inner flow aerodynamic.

E-mail: waste_wan@163.com

带放气槽的定几何二元倒置"X"型混压式超音速进气道实验研究

万大为，郭荣伟

（南京航空航天大学 能源与动力学院，江苏 南京 210016）

摘要：针对一种带放气槽的定几何二元倒置"X"型混压式超音速进气道进行了风洞吹风实验。结果表明：随着来流马赫数的增加，进气道总压恢复系数不断减小，流量系数却先增加，在设计点达到最大值后减小；当攻角变化时，两侧进气道变化各异，在小攻角 $\alpha \leqslant 6^0$ 时，随着攻角的增加，迎背风两侧进气道的总压恢复系数均有所下降，但背风侧进气道总压恢复系数高于迎风侧进气道，在流量系数方面，背风侧进气道先增加后减小，而迎风侧进气道一直保持缓慢下降，但两侧总的流量保持变化不大，在大攻角（$\alpha = 6^0$-9^0）状态下，背风侧进气道总压恢复系数和流量系数均下降剧烈，而迎风侧进气道总压恢复系数下降但流量系数却有所上升；同时，通过与不带放气槽进气道的速度特性以及反压特性对比发现，放气槽的存在不但增加了进气道的稳定工作范围，而且对进气道在高马赫数下性能的提高也大有裨益。本文为倒置"X"型进气道的设计、改进提供了实验依据。

关键词：航空、航天推进系统；超音速进气道；二元混压式；实验研究；放气槽；"X"型布局；倒置

中图分类号：V211.3 文献标识码：A

第39卷第3期 南京航空航天大学学报 Vol 39 No. 3
2007年6月 Journal of Nanjing University of Aeronautics & Astronautics Jun. 2007

定几何二元倒置"X"型混压式超声速进气道实验

万大为 郭荣伟
(南京航空航天大学能源与动力学院, 南京, 210016)

摘要: 针对一种定几何二元倒置"X"型布局的混压式进气道进行了风洞吹风实验, 得到了进气道的性能并进行了分析。结果表明, 随着来流马赫数的增加, 进气道总压恢复系数不断减小, 流量系数却先增加, 在设计点达到最大值后减小。当迎角变化时, 迎背风侧进气道呈现不同的特性, 在小迎角($\alpha < 6°$)状态下, 背风侧进气道总压恢复系数先上升后下降, 迎风侧进气道总压恢复系数却保持一直缓慢下降, 在流量系数方面, 背风侧进气道流量系数一直增加而迎风侧减小, 但两侧总的流量变化不大; 在大迎角($\alpha = 6° \sim 9°$)状态下, 背风侧进气道总压恢复系数和流量系数均下降剧烈, 而迎风侧进气道总压恢复系数虽有下降但流量系数却有所上升。本文为倒置"X"型进气道的设计提供了实验依据。

关键词: 二元混压; "X"型布局; 超声速进气道; 倒置
中图分类号: V 211.3 **文献标识码**: A **文章编号**: 1005-2615(2007)03-0277-05

Experiment on Fixed-Geometry Two-Dimensional Mixed-Compression Supersonic Inlet with Sweepforward High-Light and "X"-Type Missile Configuration

Wan Dawei, Guo Rongwei
(College of Energy and Power Engineering, Nanjing University of Aeronautics & Astronautics, Nanjing, 210016, China)

Abstract: A fixed-geometry two-dimensional mixed-compression supersonic inlet with sweepforward high-light is tested in a wind tunnel. The inlet is designed in an "X" type missile configuration. Results indicate that: (1) The total pressure recovery decreases with the increase of the free stream Mach number, while the mass flow ratio keeps increases firstly and then declines rapidly, the maximum value is obtained at the design point. (2) When the angle of attack is rised less than 6°, the total pressure recovery of the flow in the lee side inlet increases and then falls, while the windward side inlet retains decreasing; the mass flow ratio of lee side inlet keeps ascent and the windward side inlet goes down, so that the summation of both sides is almost constant. (3) When the angle of attack is rised from 6° and 9°, both the total pressure recovery and the mass flow ratio of the lee side inlet fall quickly, and the total pressure recovery of the windward side inlet also decreases, but its mass flow ratio increases. An example is provided for the design of the type inlet.

Key words: two-dimensional mixed-compression; "X" type configuration; supersonic inlet; sweepforward high-light

引 言

作为冲压发动机主要部件之一的进气道, 其设计的好坏直接影响冲压发动机的总体性能。目前, 在冲压发动机进气道中, 由于混压式兼有外阻较小和较易启动的优点[1], 在进气道设计中常被采

收稿日期: 2006-08-03; **修订日期**: 2007-02-28
作者简介: 万大为, 男, 博士研究生, 1979年12月生; 郭荣伟(联系人), 男, 教授, 博士生导师, E-mail: grwei@nuaa.edu.cn。

用[2-6]。另一方面,对于采用冲压发动机的导弹,由于弹体与进气道之间存在气动干扰,从而影响进气道的流态,因此就必须对导弹采用一体化设计。

在现行超声速弹用进气道布局方案中,"X"型布局有着广泛的应用。常用的"X"型布局的进气道主要有半圆锥型以及正置二元矩形(压缩面背靠弹身)两种形状。早在20世纪六七十年代,国外就针对这种布局进气道开展了一系列研究,且研究成果早已付诸应用,如美国的ALVRJ导弹就采用了正置二元矩形的"X"型布局,俄罗斯著名的KH-31P采用的是半圆锥型,而德国的新一代导弹A mm iger采用了4个倒置(压缩面在外侧,面对弹身)的"X"型布局二元进气道。据称该类进气道具有较好的迎角性能,但相关的研究文献未见报导。国内虽起步较晚,但也进行了一系列的研究工作,文献[6-7]采用数值方法对"X"型布局的半圆锥形和二元矩形进气道进行了分析,并指出二元矩形进气道在升阻比方面相对半圆锥进气道更具优越性。文献[8]对某正置"X"型二元矩形进气道的迎角特性进行了数值仿真研究。但这些研究主要集中在数值仿真方面,缺乏足够的实验数据支持,同时,其研究对象主要集中在国外成熟的半圆锥和正置二元矩形方面,对倒置"X"型布局的进气道尚未进行研究,因此,开展这方面研究是很有必要的。

本文针对这种情况,设计了一个采用倒置"X"型布局的的二元混压式进气道,并进行了风洞吹风实验。结果表明,小角度迎角$\alpha<6°$范围内,进气道性能对迎角不敏感,具有良好的气动特性。本研究为倒置"X"型布局进气道的设计和应用提供了实验依据。

1 实验模型与设计

本文设计的二元进气道封口马赫数为3.0,起动马赫数2.0,最大工作马赫数3.5,采用定几何混压式。两级外压缩楔板(ramp)与水平面夹角分别为10,17°,唇罩(cowl)内型面与水平面夹角为9°,进气道入口高度与喉道高度之比为2.0,喉道后扩压器部分当量扩张角约为3°,有效避免了气流分离。

1.1 实验模型

图1给出了本研究的超声速进气道实验模型示意图。进气道采用倒置"X"型布局方式,4个进气道沿弹身周向均匀分布,其楔面(ramp)尖点距弹尖距离为5倍弹身直径。自由来流经弹身前体后进入进气道,然后通过拐弯段进入掺混段掺混。实验时,通过出口的节流锥调节掺混段的压力来模拟燃烧室反压的变化。为了获得进气道的流量系数和总压恢复系数,在每个进气道扩张段结束处安装了总压测量耙。同时,在进气道的楔面(ramp)侧的壁面上布置有沿程静压孔,用以测量进气道内的沿程静压分布。

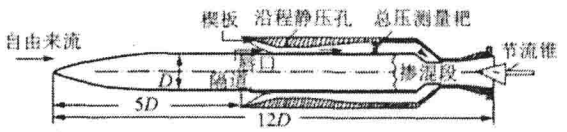

图1 进气道实验模型示意图

1.2 实验设备

实验工作是在南京航空航天大学的NH-1风洞中完成的。NH-1风洞是暂冲亚、跨、超声速风洞,马赫数范围为0.3~3.5,实验段截面尺寸为0.6 m×0.6 m。超声速实验时通过更换喷管获得不同的来流马赫数。实验段每一侧壁各有两个直径230 mm的观察窗,供纹影仪观察录像以及显示流场使用。

实验来流马赫数范围为2.0~3.5,雷诺数约为3×10^7,模型在风洞中的堵塞比约为3.4%。图2为模型在风洞中的照片。

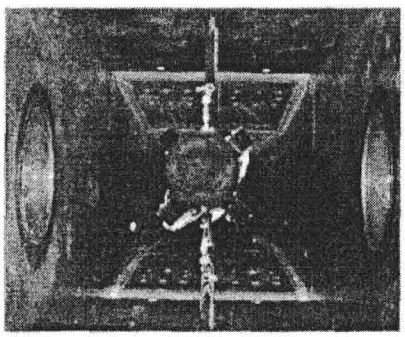

图2 进气道模型在NH-1风洞中

2 实验结果与讨论

本文通过高速风洞吹风实验研究得到了进气道的总压恢复系数、流量系数等性能参数随工作条件的变化规律以及有关状态下进气道的沿程静压分布曲线,现讨论如下。

2.1 进气道反压特性

对超声速亚燃冲压发动机而言,进气道的反压特性,不仅代表了进气道性能参数在超临界、临界以及亚临界等工作状态下的高低,而且还是发动机燃烧室设计以及进气道/燃烧室相容工作的依据。图3,4给出了本研究进气道的反压特性,分别为进

气道总压恢复系数和流量系数随进气道出口反压变化的规律($M\ a$= 3.0, α= 0°, β= 0°, γ= 45°, 以下如无特别说明, 侧滑角β和滚转角γ均分别为0°和45°)。图中纵坐标分别为总压恢复系数和流量系数, 由其临界工作状态下的对应数值归一化处理, 横坐标为进气道出口反压, 也由临界工作状态下的反压无因次化, 其中曲线中的箭头代表节流锥移动方向。可以看出, 在进气道超临界工作状态下, 随着锥位的向前移动, 出口反压上升, 结尾激波前移, 进气道总压恢复系数也随着上升, 并在临界状态达到最大值, 而此过程中由于进口激波系维持不变, 故流量系数一直保持不变; 随着锥位的进一步前移, 进气道流量系数开始下降, 对应的进气道出口反压和总压恢复系数也逐渐下降。这是由于此时对应的状态为亚临界状态, 在进气道入口处产生脱体激波而造成的。

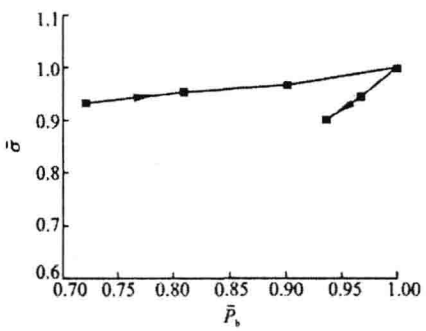

图3　总压恢复系数随进气道出口反压变化曲线

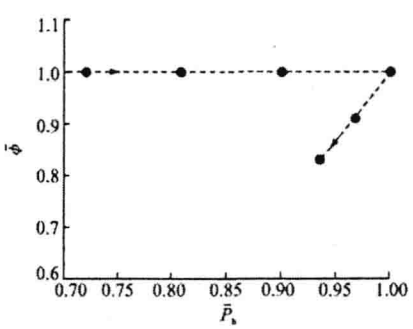

图4　流量系数随进气道出口反压变化曲线

2.2　进气道性能随来流马赫数的变化

图5给出的是当α= 0°时进气道总压恢复系数随来流马赫数的变化曲线。图中纵坐标为各个马赫数下的总压恢复数值与$M\ a$= 2.0状态下的对应数值的比值。可以看出, 随着来流马赫数的增加, 进气道总压恢复系数不断下降, 特别是在$M\ a$= 3.0后下降剧烈, 当$M\ a$= 3.5时总压恢复系数仅为$M\ a$= 2.0的40%。这是由于当来流马赫数超过设计封口马赫数后, 外压缩楔板产生的斜激波交汇在进气道唇口内, 导致滑流层进入进气道, 同时, 由于交汇后的激波与唇口附近壁面的附面层相互作用, 引起局部气流分离, 两方面的作用增大了进气道的损失, 从而使得进气道总压恢复下降剧烈。因此在设计超声速混压式进气道时应恰当地选择封口马赫数, 以保证非设计状态下的性能以及稳定工作。

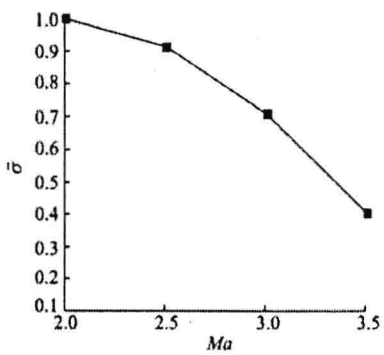

图5　α= 0°时总压恢复系数随来流马赫数变化曲线

图6给出了进气道流量系数随来流马赫数的变化曲线, 图中纵轴已按$M\ a$= 3.0状态下的流量系数作归一化处理。图中, 当来流马赫数低于封口马赫数时, 流量系数随着马赫数的增加而增大, 到$M\ a$= 3.0时达到最大值, 当来流马赫数继续增大时, 进气道流量系数反而减小, 这是由于弹头的损失不断增大, 使到达进气道入口的气流总压恢复减小较多而引起的。

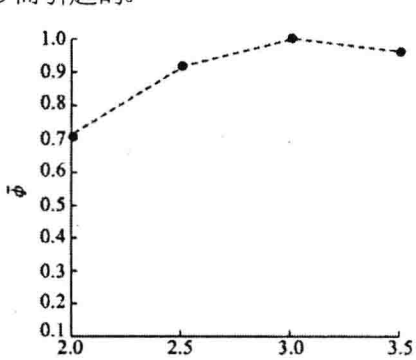

图6　α= 0°时进气道流量系数随来流马赫数变化曲线

2.3　进气道性能随来流迎角的变化

实验时以抬头迎角为正(图2), 为了简便, 本文将处于弹身迎风侧的进气道记作迎风侧进气道, 处于弹身背风侧的进气道记作背风侧进气道。图7为$M\ a$= 3.0时进气道总压恢复系数随来流迎角的变化曲线, 其纵坐标已按对应0°迎角下的总压恢复系数归一化处理。图中, 随着迎角的增加, 迎风侧进气道的总压恢复系数不断下降, 而背风侧进气道总压恢复系数在α< 3°时略有上升, 随后缓慢下降, 在α